Geodynamic Contributions to Global Climatic Change

Bruce G. Bills
Geodynamics Branch
NASA Goddard Space Flight Center
Greenbelt, MD 20771

Abstract

Orbital and rotational variations perturb the latitudinal and seasonal pattern of incident solar radiation, producing major climatic change on time scales of 10^4-10^6 years. The orbital variations are oblivious to internal structure and processes, but the rotational variations are not. The intent of this article is to describe a program of investigation whose objective would be to explore and quantify three aspects of orbital, rotational and climatic interactions. An important premise of this investigation is the synergism between geodynamics and paleoclimate. Better geophysical models of precessional dynamics are needed in order to accurately reconstruct the radiative input to climate models. Some of the paleoclimate proxy records contain information relevant to solid Earth processes, on time scales which are difficult to constrain otherwise.

Specific mechanisms which will be addressed include:

- climatic consequences of deglacial polar motion, and
- precessional and climatic consequences of
  - glacially induced perturbations in the gravitational oblateness, and
  - partial decoupling of the mantle and core.

The approach entails constructing theoretical models of the rotational, deformational, radiative and climatic response of the Earth to known orbital perturbations, and comparing these with extensive records of paleoclimate proxy data. Several of the mechanisms of interest may participate in previously unrecognized feed-back loops in the climate dynamics system. A new algorithm for estimating climatically diagnostic locations and seasons from the paleoclimate time series is proposed.

INTRODUCTION

It is widely recognized that mass redistributions associated with climatic change (glaciations) are an important source of crustal deformation and geodynamic change. It is much less widely appreciated that rates, phases and amplitudes of deformation of the deep interior of the Earth can influence climate. The objective of this investigation is to better characterize four aspects of this geodynamic contribution to global climatic change. The common theme among them has two threads: internal mass redistributions influence the rotational dynamics of the Earth, and changes in orbital and rotational parameters influence the latitudinal and seasonal pattern of insolation. Previous attempts to account for astronomically forced climatic change have usually only considered extremely simplisitic models for the response of the Earth to external torques and surface loads.

The focus of the proposed investigation will consist of three specific aspects of interaction between internal mass flow and rotational dynamics, and a new algorithm for comparing paleoclimatic proxy data with astronomically forced variations in insolation patterns.

The latitudinal and seasonal pattern of incident solar radiation depends on the eccentricity of the Earth's orbit and the orientation of the spin axis relative to both the orbit normal and the aspidal line. Unit vectors $\mathbf{s}$ and $\mathbf{n}$ characterize the directions of the spin axis and orbit normal, respectively. Two angles completely characterize the relative orientation of the spin axis. The obliquity ϵ is simply the angle between the orbit normal and the spin axis

$$\epsilon = cos^{-1}(\mathbf{n} \cdot \mathbf{s}) \tag{1}$$

The ascending node of the orbit plane on the instantaneous equator plane has an orientation given by $(\mathbf{s} \times \mathbf{n})$, and the longitude of perihelion ϖ is just the angle in the orbit plane from that node to perihelion. It is widely appreciated that secular variations in these three parameters (e,ϵ,ϖ) produce major climatic change (Hays et al., 1976; Berger et al., 1984). In fact, spectral analyses of long, high resolution marine sediment isotopic records show significant variance at periods near 100 kyr, 41 kyr and 19-23 kyr, which are generally attributed to spectral lines in the radiative forcing fluctuations associated with e, ϵ and e sin(ϖ), respectively.

The causes and effects of the orbital changes are quite well understood. Gravitational interactions with the other planets cause the shape and orientation of the orbit to change on time scales of 10^4-10^6 years. The inclination I and nodal longitude Ω determine the orientation of the orbit plane. The eccentricity e and perihelic longitude ω determine the shape of the orbit and its orientation within the plane. Note that ω is measured from an inertially fixed direction, rather than the moving

node as is the case for ϖ. The secular evolution of the orbital element pairs (I,Ω) and (e,ω) can be conveniently represented in terms of Poisson series

$$\begin{aligned} p &= sin(I)\ sin(\Omega) &&= \Sigma N_j\ sin(s_j\, t + g_j) \\ q &= sin(I) cos(\Omega) &&= \Sigma N_j\ cos(s_j\, t + g_j) \end{aligned} \tag{2}$$

$$\begin{aligned} h &= e\ \sin(\omega) &&= \Sigma M_j\ sin(r_j\, t + f_j) \\ k &= e\ \cos(\omega) &&= \Sigma M_j\ cos(r_j\, t + f_j) \end{aligned} \tag{3}$$

In the lowest order solution, there are as many frequencies r_j and s_j as there are planets. However, the frequencies r_j and s_j are characteristic modal frequencies (eigenvalues) of the coupled system of oscillators and are not each uniquely associated with a particular planet (Milani, 1988). The frequencies r_j are all positive, indicating that the perihelia advance. In the lowest order solution, the apsidal rates are all in the interval ($0.667 < r_j < 28.221$ arcsec/year). The corresponding periods are 45.92 kyr to 1.943 Myr. One of the frequencies s_j is zero, and all the others are negative, indicating that the nodes regress. In the lowest order solution, the non-zero nodal rates are all in the interval ($0.692 < s_j < 26.330$ arcsec/year). The corresponding periods are 49.22 kyr to 1.873 Myr. In higher order solutions, variations in (e,ω) become coupled to variations in (I,Ω), but the solutions can still be cast in terms of Poisson series like Equations (2) and (3).

Laskar (1988) has recently published a secular variation theory which is complete to fifth order in eccentricity and inclination. Agreement between this secular variation model and strictly numerical computations (Richardson and Walker, 1989; Quinn et al., 1991) is much better than for any previous analytical model. The inclination and eccentricity series for Earth each contain 80 distinct terms. Figures (1) and (2) illustrate the spectra and corresponding histories of variation in orbital inclination and eccentricity for the past 2 10^6 years.

In computing these secular orbital variations, the Earth, Moon and planets can all be treated as point masses. No internal structure or processes are relevant to orbital evolution. The physics of the process is simple, and well understood, though development of proper mathematical tools to represent the long term evolution remains an area of active research (Laskar, 1988, 1990; Quinn et al., 1991). On the other hand, the rotational evolution does depend rather sensitively on various aspects of the structure and dynamics of the interior.

Lunar and solar gravitational torques acting on the oblate figure of the Earth cause the spin axis $\mathbf{s}$ to precess about the instantaneous orbit normal $\mathbf{n}$. If the Earth is considered to be a rigid body,

the evolution of the spin axis orientation is given by

$$ds/dt = \alpha(\mathbf{n} \cdot \mathbf{s})(\mathbf{s} \times \mathbf{n}) \tag{4}$$

where

$$\alpha = \frac{3(C-A)}{2Cn} \sum \frac{Gm_i}{b_i^3}\{1 - 3sin^2(I_i)\} \tag{5}$$

is a scalar rate factor which depends on intrinsic properties of the Earth, such as polar and equatorial moments of inertia (C,A) and rotation rate n, and on extrinsic influences, such as masses m, orbital inclinations I, and semiminor axes b, of the Moon and Sun. The solar and lunar torques together produce a precession of the spin axis of the Earth at a rate of $\alpha(\mathbf{n} \cdot \mathbf{s}) = 50.38$ arcsec/year (Kinoshita, 1977, Williams et al., 1991).

Once the present spin axis direction s is known and orbital element histories are given via Equations (2) and (3), an obliquity history can be constructed from equation (4) in two different ways. The linear perturbation approach (Miskovic, 1931, Sharaf and Boudnikova, 1967; Vernekar, 1972, 1977; Ward, 1974; Berger, 1976) involves deriving coefficients of a trigonometric series, similar to Equations (2) and (3), which yield the obliquity and longitude of perihelion directly as functions of time. An alternative is to apply standard numerical algorithms for solving initial value problems to generate a vector time series s(t) and then compute the obliquity and longitude of perihelion directly (Ward, 1979; Laskar, 1986; Bills, 1990b). Figure (3a) shows the spectrum of obliquity variations, which in the linear perturbation model is simply obtained from the inclination spectrum by shifting each frequency s_j by the luni-solar precession rate (s = 50.38 arcsec/year) and multiplying each amplitude N_j by the spectral admittance

$$F_j = s_j/(s_j + s) \tag{6}$$

Figure (3b) shows the numerically integrated obliquity history of Laskar (1986,1988) for the last 2 Ma, using the rotational theory of Kinoshita (1977). The difference between the numerical and linear perturbation solution never exceeds 0.06 degree over that interval. It is clear that the linear perturbation solution gives a very adequate representation of the spin precession.

The influence of orbital and rotational variations on climate is operative through perturbations in the latitudinal and seasonal pattern of insolation. The diurnal average intensity of radiation at a point is inversely proportional to the squared solar distance and directly proportional to the diurnal average rectified solar direction cosine

$$F = (a/r)^2 \langle ||\mathbf{u} \cdot \mathbf{u}_s|| \rangle \tag{7}$$

where a and r are mean and instantaneous solar distance and $\mathbf{u}$ and $\mathbf{u}_s$ are unit vectors from the center of the Earth to the surface point of interest and the sub-solar point, respectively. The insolation pattern, as a function of latitude θ and mean anomaly M, can be readily computed once values are specified for the orbital and rotational parameters ϵ, e, and ϖ (Hargreaves, 1895; Milankovitch, 1920; Vernekar, 1972, 1977; Ward, 1974). Figure (4) illustrates that pattern for the present orbital and rotational configuration. This pattern can also be written in terms of a Fourier-Legendre series (Hargreaves, 1895; North and Coakley, 1979; Taylor, 1984; Bills, 1992)

$$F(\mu, M; \epsilon, e, \varpi) = \sum P_n(\mu) \sum exp(ip\,M)\; F_{n,p}(\epsilon, e, \varpi) \tag{8}$$

where $\mu = \cos(\theta)$, and P_n is a Legendre polynomial. The number of terms in the Fourier summation required to obtain a good representation of the seasonal pattern is greater in the polar regions than in the tropics and mid-latitudes. The primary difficulty in the polar regions is reproducing the abrupt change in slope of the insolation curve at times of transition to continual darkness or continual light. It is also true that the polar regions place the greatest demands on the Legendre summation, since the spatial pattern also has a discontinuous first derivative at the latitude where the transition occurs to continual darkness or light.

A significant fraction of the recent work on comparing paleoclimate proxy records to astronomically forced insolation changes has been based on the published insolation curves of Berger (1978, 1991). Common practice is to compare computed variations in some particular aspect of the seasonal and latitudinal insolation pattern (July insolation at 65° N is a particularly frequent choice) with an observational record of some climatic indicator ($\delta^{18}O$ variations versus age (depth) in a marine sediment core, for example). Comparisons of this sort enable estimates of amplitude, phase and coherence of climatic response to radiative forcing, and have unequivocally demonstrated that orbital and rotational variations are a dominant cause of climatic change on time scales of 10^4-10^6 years.

Despite obvious successes, several problems remain in the general methodology. For example, the orbit and rotation are both assumed to be perfect clocks and, as a result, data time series are often "tuned" to the astronomical time scale (Martinson et al., 1982; Shackleton et al., 1990; Hilgren, 1991). However, as we shall see in the next two sections, the rotational variations in particular do not keep very good time. Also, a number of significant observations remain without adequate explanation. One of the most perplexing of these is the mid-Pleistocene climatic switch in dominant oscillation frequency. The 41 kyr oscillation was dominant throughout the early Pleistocene, and the 100 kyr oscillation has been dominant since the Brunhes-Matuyama magnetic polarity reversal

(or thereabouts), whereas the standard July 65° N insolation curve shows no discernible change in spectral composition over the entire interval.

The intent of this article is to point out the need for a critical examination of this standard scenario, with the objective of improving the geodynamic component of the model enough to provide better radiative forcing time series to the paleoclimate community, use paleoclimate proxy data records to calibrate solid earth responses to applied loads and torques, and explore potential feed-back loops .

Two of the topics of study are perturbations to the simple precession model presented in Equation (4). The first topic concerns time variations in the precession rate occasioned by glacial mass transport and resulting changes in the difference between polar and equatorial moments of inertia (C-A). These fractional variations can likely reach 1% in magnitude and are fully competitive with changes in orbital eccentricity in terms of their effect on instantaneous precession rate. The second topic is the effect of differential precession in the deep interior, which is governed by the (poorly known) characteristics of the inertial and dissipative coupling torques which attempt to keep the rotation axes of the mantle and core aligned.

The third topic is the potentially significant geodynamic feed-back loop associated with deglacial mass transport, polar motion and ensuing perturbations to radiative equilibrium temperature patterns. The asymmetrical disposition of major ice sheets and ocean basins relative to the rotation axis implies that during growth or decay of these ice sheets the geographic location of the principal axis of greatest inertia will shift. If the hydrospheric and cryospheric changes are appreciably more rapid than can be compensated by asthenospheric flow, the rotation axis will shift, possibly by as much as ~ 1°. The primary climatic consequence is a shifting of the geographic distribution of continental and oceanic regions (which differ by a factor of 60 in heat capacity). The effect of a 1° change in the geographic position of the pole is different (but not necessarily less significant) than a 1° change in obliquity.

The fourth and final topic is a new modelling strategy in which climate proxy data records are used to estimate linear combinations of insolation pattern Fourier-Legendre coefficients which best duplicate the observed variations. This approach allows the data variance to be partitioned into global versus regional effects, and can distinguish between responses to annual average insolation and those due to seasonal cycle fluctuations.

PRECESSIONAL DYNAMICS WITH VARIABLE RATE FACTOR

Statement of Problem

All but the most recent reconstructions of the radiative forcing input to paleoclimate models have assumed that both the orbital and rotational dynamics could be readily and accurately reconstructed from their present configurations, via the simple analyses mentioned in the introduction. These expectations seem well founded in the case of orbital evolution, though the possibility of chaotic dynamics in the inner solar system (Laskar, 1990; Laskar et al., 1992) does seem to preclude confident extrapolation beyond 10^7 years. However, there are a number of processes, working in different locations and at different rates, which all serve to compound the difficulty of accurately computing the spin precessional evolution.

An important aspect of this problem is the synergism between geodynamics and paleoclimate. Better geophysical models are needed in order to accurately reconstruct the radiative input to climate models. Some of the paleoclimate proxy records contain information relevant to solid Earth processes on time scales which are difficult to constrain otherwise.

On the longest time scales of interest (10^7-10^9 years) the limiting uncertainty is variability in the tidal transfer of angular momentum from the rotation of the Earth to the orbit of the Moon. At present, these tidal torques are increasing the length of the day by 22.5 10^{-6} sec/year and increasing the size of the lunar orbit by 3.88 cm/year (Cazenave and Daillet, 1981; Christodoulidis et al., 1988). Berger et al. (1989) have made a useful first step towards including this effect in climatic time series. They computed the change in the major precession and obliquity frequencies due to lunar tidal evolution, assuming that the present rate of tidal energy dissipation is representative of the past 500 Myr. However, the present rates are considerably higher than the long term average (Hansen, 1982), largely due to a near resonance between sloshing modes of ocean basins and the diurnal and semidiurnal tidal periods (Platzman et al., 1981), and apparently compounded by a contribution from shallow seas (Wunsch, 1986; Dickman and Preisig, 1986). Sedimentary records which constrain lunar orbital evolution show some promise of resolving this problem (Olsen, 1986; Williams, 1989a,b; Herbert and D'Hondt, 1990), but the situation is definitely more complex than is suggested by Berger et al., (1989).

Another parameter which can vary, on rather shorter time scales and in an equally irregular

fashion, is the gravitational oblateness of the Earth (C-A)/C. Thomson (1990) has recently made three important contributions to the understanding of this source of variability. First, he pointed out that mass redistribution associated with major glaciations and compensating subsidence and crustal deformations (Le Treut and Ghil, 1983; Wu and Peltier, 1984) can cause fractional changes in oblateness of order 10^{-3}-10^{-2}. Second, he showed that high resolution spectral analyses of several climatic time series appear to indicate fluctuations of the luni-solar precession rate of this magnitude, and with a dominant period near 100 kyr. Finally, Thomson pointed out that the best fit to the paleoclimate proxy data was obtained using a mean lunisolar precession rate 0.6 arcsec/year less than the present observed value. He notes that the resulting value would correspond rather closely with that expected for a hydrostatic flattening (Nakiboglu, 1982). If these important results are corroborated, they will demonstrate that important feed-back loops exist in the orbital-rotational-climatic interactions system, further "up-stream" in the presumed causal chain than has been previously recognized.

Approach

The research design for this segment of the proposed investigation will address several issues. The primary focus will be an attempt to resolve two related questions. What are the precessional and paleoclimatic consequences of small (0.001-0.01) variations in oblateness (C-A)/C, over time scales of 10^3-10^6 years? Can such variations can be confidently inferred from paleoclimatic proxy data? These questions represent a forward modeling problem and a coupled inverse problem, respectively.

The first question is the easier to answer. Equation (4) describes the variations in orientation of the spin axis, as viewed in an inertial reference frame. However, since we are primarily interested in the orientation of the spin axis relative to orbit normal (obliquity) and the apsidal line (longitude of perihelion), the analysis will be made easier if we first transform to a coordinate system fixed in the orbit plane. If the rotation matrix is denoted by A, the transformed equation takes the form (Ward, 1974; Bills, 1990a)

$$d\mathbf{s}/dt = \{dA/dt\ A^{-1}\}\mathbf{s} + a(\mathbf{n}\cdot\mathbf{s})(\mathbf{s}\times\mathbf{n}) \tag{9}$$

where

$$\{dA/dt\ A^{-1}\} = B\ dI/dt + C\ dW/dt \tag{10}$$

$$B = \begin{bmatrix} 0 & 0 & 0 \\ 0 & 0 & 1 \\ 0 & -1 & 0 \end{bmatrix} \tag{11}$$

$$C = \begin{bmatrix} 0 & \cos(I) & -\sin(I) \\ -\cos(I) & 0 & 0 \\ \sin(I) & 0 & 0 \end{bmatrix} \tag{12}$$

Now define two complex quantities: P = sin(I) $e^{i\Omega}$, which represents components of the orbit normal on the invariable plane, and S = sin(ϵ) $e^{i\Psi}$, which represents components of the spin vector on the orbital plane. In this new notation, Equation (9) can be rewritten in the form

$$dS/dt + ia\ S = ib\ dP/dt \tag{13}$$

where

$$a = \alpha cos(\epsilon) + cos(I)\ d\Omega/dt \tag{14}$$

$$b = cos(\epsilon)e^{-i\Omega} \tag{15}$$

The complete solution to a nonhomogeneous linear differential equation consists of both "free" and "forced" modes of oscillation. The free modes, in this case, correspond to spin precession with the orbit plane fixed, and the forced modes correspond to motions of the spin axis as it attempts to precess about the instantaneous orbit normal, while the orbit normal itself is precessing. The forced modes make first order contributions to both ϵ and ϖ, whereas the free modes are only second order for ϵ but are first order for ϖ. As a result, in the standard linear series solutions (Berger, 1978; Ward, 1974), the obliquity terms include only the forced response to changes in (I,Ω), whereas the nodal longitude terms include both forced modes from (I,Ω), and free modes with variable (e,ω).

The result of variable oblateness will have exactly the same qualitative effect on spin precession as does a change in orbital eccentricity. Both effect the free modes only. It will thus be rather difficult to confidently distinguish oblateness variations from unmodeled eccentricity variations. However, that does not effect the forward modeling aspect of the problem. To the extent that oblateness variations occur, their effect should be included in the astronomical forcing to climate models.

An iterative approach to the problem seems promising. Orbital variations are uneffected by oblateness and need not directly concern us. As a first step, standard rotational variations (including eccentricity, but neglecting oblateness variations) will be used to generate radiative input to an energy balance climate model (North et al., 1981; Short et al., 1991), with a coupled ice-sheet model

(DeBlonde and Peltier, 1990). Time variations in oblateness can be simply estimated from the surface load and internal compensation. The resulting oblateness history is then fed back into the rotational calculation and the entire process is repeated. The inner-most loops of this algorithm are somewhat similar to the model of Peltier (1982). However, he did not allow the mass loading to influence the radiative forcing.

Even fairly modest changes in oblateness are rotationally significant. For comparison, the eccentricity perturbation influences precession rate via the factor $(a/b)^3$, where a and b are semimajor and semiminor axes, respectively. This amounts to $(1\text{-}e^2)^{-3/2}$, which differs from unity by only 0.0054 for a near-maximum value of $e = 0.06$,

DIFFERENTIAL PRECESSION: INERTIAL AND DISSIPATIVE COUPLING OF THE MANTLE AND CORE

Statement of Problem

The hydrostatic figure of a planet represents a compromise between gravitation, which attempts to attain spherical symmetry, and rotation, which prefers cylindrical symmetry. Due to its higher mean density, the core of the Earth is more nearly spherical than the mantle. The direct luni-solar precessional torques on the core will thus be inadequate to make it precess at the same rate as the mantle. In fact, the core oblateness is only about 3/4 that required for coprecession with the mantle (Smith and Dahlen, 1981). However, it is clearly the case that the core and mantle precess at very nearly the same rate (Stacey, 1973). A variety of different physical mechanisms contribute to the torques which achieve this coupling, but a purely phenomenological partitioning is useful. The net torque can be described as a sum of inertial torques, which are parallel to $(\chi_m \times \chi_c)$, and dissipative torques, which are parallel to $(\chi_m - \chi_c)$. Here, χ_c and χ_m are the rotation vectors of the core and mantle, respectively. The two types of torques have qualitatively different results: inertial torques cause the core and mantle axes to precess at fixed angular separations and on opposite side of their combined angular momentum vector, whereas the effect of dissipative torques is to reduce the angle between the axes.

On short time scales it is appropriate to consider the core to be an inviscid fluid constrained to move within the ellipsoidal region bounded by the rigid mantle (Poincare, 1910; Toomre, 1966; Voorhies, 1991). The inertial coupling provided by this mechanism is effective whenever the ellipticity of the container exceeds the ratio of the precessional to rotational rates. If the mantle were actually rigid, or even elastic (Merriam, 1988; Smylie et al., 1990), this would be an extremely effective type of coupling. However, on sufficiently long time scales, the mantle will deform viscously and can accommodate the motions of the core fluid (Wu, 1990). The inertial coupling torque exerted by the core on the mantle will have the form

$$T_i = k_i[\chi_m \times \chi_c] \tag{16}$$

A fundamentally different type of coupling is provided by electromagnetic or viscous torques (Rochester, 1962; Sasao et al., 1977; Kubo, 1979). The dissipative coupling torque exerted by the

core on the mantle will have the form

$$T_d = k_d[\chi_m - \chi_c] \tag{17}$$

This type of coupling is likely to be most important on longer time scales. In each case, the mantle exerts an equal and opposite torque on the core. The response of the coupled core-mantle system to orbital forcing is given by (Goldreich and Peale, 1970; Ward and DeCampli, 1979; Bills, 1990b).

$$\begin{aligned} ds_m/dt &= \alpha_m(n \cdot s_m)(s_m \times n) - \beta_m(s_m - s_c) - \gamma_m(s_m \times s_c) \\ ds_c/dt &= \alpha_c(n \cdot s_c)(s_c \times n) + \beta_c(s_m - s_c) + \gamma_c(s_m \times s_c) \end{aligned} \tag{18}$$

where α_m is similar to α above, except that only mantle moments A_m and C_m are included, and

$$\begin{aligned} \beta_m &= k_d/C_m\,\upsilon \\ \gamma_m &= k_i/C_m\,\upsilon^2 \end{aligned} \tag{19}$$

where υ is the mean rotation rate.

Approach

The research design for this segment of the proposed investigation would consist of several parts. The objectives and methods are very similar to those described in the previous section. In this case, however, the intent would be to determine the precessional and paleoclimatic consequences of non-rigd core-mantle coupling, and to explore the possibility that useful constraints on the coupling parameters can be obtained from paleoclimatic proxy data.

A number of estimates already exist for the strengths of inertial and dissipative coupling torques (Toomre, 1966; Roberts, 1972; Rochester, 1976; Loper, 1975; Stix, 1982). By most accounts, the inertial torque is ~ 5 10^{20} N m, and the various viscous and magnetic dissipative torques are 102-104 times weaker. However, the inertial torque estimates are simply based on the premise that the core must coprecess with the mantle.

Solutions to the coupled precession problem can be found in a form analogous to Equation (11) for the rigid precession problem. The principle difference in the present situation is the increased richness of the free and forced oscillation spectra. There are modes in which the core and mantle precess together, and other modes which reflect differential precession. It is clear that the most climatically relevant behavior is the precessional motion of the mantle. Thus the chief interest, from that perspective, will be to explore the behavior of the mantle precession modes over plausible range of parameter values. Within the geophysically prescribed range of parameter space, are there any

climatically significant perturbations to obliquity or longitude of perihelion occasioned by partially decoupling the core from the mantle?

It is very clear that the mantle and core exhibit differential motions on nutational time scales (Mathews et al., 1991; Mathews and Shapiro, 1992). However, one of the difficulties in constructing a differential precession model which is truly useful for paleoclimatic studies is that the precise geodetic techniques, which are able to constrain nutation amplitudes within a few milliarcseconds, still have short enough time spans that most of the differential precession modes of interest are still indistinguishable from rigid rotation.

DEGLACIAL POLAR MOTION AND ABRUPT CLIMATE CHANGE

Statement of Problem

Recent models of the surficial mass transport associated with the last deglaciation (Tushingham and Peltier, 1991; Nakada and Lambeck, 1988) suggest that the magnitude of the flow and its departure from axial symmetry were both great enough that, if it were not closely balanced by internal flow and deformation, it would cause a shift in the body-fixed location of the axis of greatest inertia, by an amount of order 1o. If the pole were to move by a significant fraction of a degree, the resulting displacement of the geographic pattern of land and water relative to the incident radiation pattern would cause a climatic perturbation which could either augment or retard the progress of deglaciation, depending on the spatio-temporal pattern of the perturbation. The potential thus exists for a previously unexplored feed-back loop in the climate system.

During the peak of the last deglaciation, there was a brief but significant return to full glacial conditions. This Younger Dryas climatic event is perhaps best documented in the North Atlantic (Ruddiman and McIntyre, 1981; Broecker et al., 1988), but appears to have been global in scale (Currey, 1990; Engstrom et al., 1990; Gasse et al., 1991). Though the broad scale timing of the deglaciation is consistent with astronomical forcing, the Younger Dryas perturbation was too brief to be a linear response to the classical orbital or rotational variations. However, neither the magnitude nor duration is a priori inconsistent with a response to deglacial polar motion. The objective of this portion of the proposed investigation would be to examine the geodynamic and climatic consequences of deglacial mass flow.

Approach

The usual geodynamic modeling approach to deglacial polar motion is to use historical observations of the rate and direction of polar motion during this century, in conjunction with estimates of the surficial mass flow, to derive constraints on deep Earth structure models. However, these same models, once they have been calibrated, can be made to deliver estimates of the rates and directions of polar motion which occurred during the deglaciation. The magnitude of deglacial polar motion depends rather sensitively on the rate and spatial pattern of surficial mass transport and on the

internal structure of the Earth, as reflected in the spectrum of relaxation times for surficial loads and body forces (Sabadini et al., 1982; Wu and Peltier, 1984; Spada et al., 1992; Ivins et al., 1992).

A class of climate models which is very well suited to the proposed investigations incorporates spatial and temporal variations in a number of components of the global energy balance. The basic equation which governs the energy balance is (North et al., 1981)

$$A + B\,T + C\,\frac{\partial T}{\partial t} - \nabla \cdot (D\,\nabla T) = Q\,a\,F \tag{20}$$

The first two terms on the left parameterize outgoing radiation, the third term represents storage of heat and the fourth term represents divergence of the heat flux. The right hand side is the amount of incident radiation that gets absorbed.

Values for the outgoing radiation parameters (A = 210 W m^{-2}, B = 2.1 W m^{-2} K^{-1}; Short et al., 1984) can be estimated from satellite data. The heat capacity C is large over water and small over land (C_w/B = 4.6 years, C_l = C_w /60; North and Coakley, 1979). Though much of the lateral transport of heat is accomplished by winds and ocean currents, these effects can be modeled by a diffusive transport, with D/B = 0.310 (North, 1975; Wyant et al., 1988). For the incident radiation, Q = S/4 = 342 W m^{-2} (Schatten and Orosz, 1990), F is the spatial and temporal pattern of projected area, and a (0.75, Stephens et al., 1981) is the co-albedo.

Solutions to this equation with specified forcing can be readily obtained in the spectral domain, with spatial patterns represented by spherical harmonic series and temporal patterns represented by Fourier series. If A, B and D are assumed to be constants (no spatial or temporal variations), the base state solution to Equation (20) is simply

$$T_{nmp} = W^{-1}[Q\,G\,a_{nmp}\,F_{n0p}] \tag{21}$$

where G (whose 9 indices have been suppressed for typographical clarity) is a coupling constant for products of spherical harmonics (Rotenberg et al., 1959; Dill, 1991) and

$$W = [B + n(n+1)\,D + i\,p\,G\,C_{nmp}] \tag{22}$$

In the same notation, the temperature perturbation δT due to a small change in radiative forcing δF (associated with ϵ, e, or ϖ) is

$$\delta T_{nmp} = W^{-1}[Q\,G\,a_{nmp}\,\delta F_{n0p}] \tag{23}$$

Similarly, the temperature perturbation due to a change δC in the distribution of land and water

relative to the rotation axis (associated with deglacial polar motion) is

$$\delta T_{nmp} = W^{-1}[-i\,p\,G\,\delta C_{nmp}\,T_{nmp}] \tag{24}$$

Specific questions which should be addressed include:

- What is the likely history (magnitude and direction) of polar motion induced during deglaciation?
- How does the climatic impact of that polar motion compare in magnitude and spatio-temporal pattern with the impact of a 1° change in obliquity, or a 1% change in orbital eccentricity?
- Is the timing and magnitude of the climatic impact such that it would significantly perturb the deglaciation?
- Is this feed-back loop a viable contributor to the Younger Dryas climatic event?

FOURIER, LEGENDRE, AND MILANKOVITCH: ESTIMATING DIAGNOSTIC SEASONS AND LATITUDES FROM CLIMATE PROXY RECORDS

Statement of Problem

As was mentioned in the introduction, a weakness of previous paleoclimate models is the common practice of using an overly simplistic representation of the insolation forcing (values for July at 65° N are a particular favorite) when attempting to reconcile computed variations in orbital and rotational parameters with observed climate proxy records (Hays et al., 1976). An alternative approach, which shares many of the same problems is to use a linear combination of the orbital and rotational parameters as input to the models (Imbrie and Imbrie, 1980). A problem in using either a linear combination of orbital and rotational parameters, or a localized spatio-temporal measure of insolation, as a proxy input to climate models is the difficulty in choosing which single value to use (Broecker, 1966; Broecker and Van Donk, 1970). Furthermore, the two alternative formats for making the choice (time and location versus orbital and rotational parameter combination) are not equivalent. It is clear that choice of a specific latitude and time of year to represent the insolation pattern implies a unique (though non-linear) combination of orbital and rotational parameters. However, the converse is not necessarily true. For some combinations of (ϵ,e,ϖ) there is no corresponding location and time of year, at which the insolation pattern will be dominated by the selected combination of parameters.

In comparing calculated insolation pattern variations with an observed time series of some climate proxy (marine sediment oxygen isotope variations, for example), it is useful to have a simple physical model in mind. The observed isotopic anomalies are, to first order, due to two effects; global ice volume fluctuations and local to regional scale temperature variations (Emiliani and Shackleton, 1974; Kahn et al., 1981). These effects differ in two important ways. The ice volume effect is global in scale and its first time derivative should be proportional to insolation driven temperature changes. In contrast, the direct isotopic temperature effect is local to regional in scale, and is directly proportional to insolation driven temperature changes.

Approach

A modeling strategy which addresses several of these points involves estimating the linear combination of Fourier-Legendre coefficients of the insolation pattern which best reproduces the data records. This approach provides the opportunity to partition observed variations into global and regional effects. It also provides information on which aspects of the insolation pattern variations are most diagnostic of the observed proxy variations. If July insolation at 65° N is truly significant in a particular data record, the selected amplitudes for the Fourier-Legendre coefficients should clearly reflect that fact. Alternatively, if the amplitude of the seasonal cycle in the polar regions or tropics, or the annual mean equator to pole insolation contrast, or any other linear functional of the insolation pattern is most diagnostic, the analysis will indicate that fact.

As an example of a situation in which this approach could be used, Park and Maasch (1992) have recently compared the climate proxy record provided by $\delta^{18}O$ records from two long, high resolution cores (ODP 677 from the eastern equatorial Pacific (Shackleton et al., 1990) and DSDP 607 from the mid-latitude North Atlantic (Ruddiman et al., 1989; Raymo et al., 1989) with a new estimate of insolation at 65° N (Berger and Loutre, 1991). The three data records analyzed (benthic and planktonic records at ODP 677, benthic only at DSDP 607) have much in common, but there are also interesting, and possibly significant, differences. It is clear that variations which are common to several locations are more likely diagnostic of global climatic variations. Differences between locations, or differences between benthic and planktonic records at a single location provide a different and complementary view of the climatic response to insolation forcing. Figure (5) illustrates a 2 10^6 year history of variations in the amplitudes of the Fourier-Legendre coefficients and Figure (6) compares the DSDP 607 and ODP 677 data with a standard insolation curve.

Several specific questions should be addressed. The first category of questions relate to calibration and characterization of technique.

- Do the Fourier-Legendre coefficient time series form an orthogonal basis?
- What output time series would correspond to a spatio-temporal delta function (summer solstice at 65° N, for example)?
- What is the resolution ($\Delta\mu$,ΔM) versus data series length?
- How does the resolution depend on other factors besides the data string length?

- Are two short data strings from significantly different locations better than a single data string of equivalent aggregate length?

The next level of question pertains to the physical meaning or significance of a particular linear combination of Fourier-Legendre coefficients. Any such linear combination is equivalent to a spatio-temporal pattern of some sort. The result obtained with a finite resolution data structure will represent the convolution of the actual physical response with the data resolution kernel. How do errors in data chronologies map into errors in resolved spatio-temporal patterns of diagnostic insolation?

The final level of question relates to understanding the implications and significance of results obtained by this algorithm from actual data series.

- Using a variety of oceanic and continental paleoclimatic data series, what are the resolved patterns of climatically diagnostic insolation?
- What physical mechanisms are implicated?
- Are significantly different patterns obtained from data strings of different age?
- Is there a single pattern which duplicates the observed increase in amplitude of the 100 kyr signal after the Brunhes-Matuyama magnetic reversal?

REFERENCES

[1] Berger, A.L. (1976), Obliquity and precession for the last 5 million years, Astron. Astrophys. 51, 127-135.

[2] Berger, A.L. (1978), Long-term variations of caloric insolation resulting from the Earth's orbital elements, Quat. Res. 9, 139-167.

[3] Berger, A.L. and M.F. Loutre (1991), Insolation values for the climate of the last 10 million years, Quat. Sci. Rev. 10, 297-317.

[4] Berger, A.L., J. Imbrie, J.D. Hays, G.J. Kukla, and B. Saltzman (1984), Milankovitch and Climate, D. Reidel, Dordrecht, 895 pp.

[5] Berger, A.L., M.F. Loutre, and V. Dehant (1989), Influence of the changing lunar orbit on the astronomical frequencies of pre-Quaternary insolation patterns, Paleocean. 4, 555-564.

[6] Bills, B.G. (1990a), Rigid body obliquity history of Mars, J. Geophys. Res. 95, 14,137-14,153.

[7] Bills, B.G. (1990b), Obliquity histories of Earth and Mars: Influence of inertial and dissipative core-mantle coupling, Lunar Plan. Sci 21, 81-82.

[8] Bills, B.G. (1992), The influence of orbital and rotational variations on latitudinal and seasonal patterns of insolation, Clim. Dynam. (submitted),.

[9] Broecker, W.S. (1966), Absolute dating and the astronomical theory of glaciation, Science 151, 299-304.

[10] Broecker, W.S., and J. Van Donk (1970), Insolation changes, ice volumes, and the O^{18} record in deep-sea cores, Rev. Geophys. Space Phys. 8, 169-197.

[11] Broecker, W.S., M. Andree, W. Wolfi, H. Oeschger, G. Bonani, J. Kennett, and D. Peteet (1988), The chronology of the last deglaciation: Implications for the cause of the Younger Dryas event, Paleocean. 3, 1-19.

[12] Cazenave, A.., and S. Daillet (1981), Lunar tidal acceleration from Earth satellite orbit analysis, J. Geophys. Res. 86, 1659-1663.

[13] Christodoulidis, D.C., D.E. Smith, R.G. Williamson, and S.M. Klosko (1988), Observed tidal braking in the Earth/Moon/Sun system, J. Geophys. Res. 93, 6216-6236.

[14] Currey, D.L. (1990), Quaternary paleolakes in the evolution of semidesert basins, with special emphasis on Lake Bonneville and the Great Basin, Paleogeo. Paleoclim. Paleoecol. 76, 189-214.

[15] DeBlonde, G. and W.R. Peltier (1990), A model of late Pleistocene ice sheet growth with realistic geography and simplified cryodynamics and geodynamics, Clim. Dynam. 5, 103-110.

[16] Dickman, S.R., and J.R. Preisig (1986), Another look at the North Sea pole tide dynamics, Geophys. J. 87, 295-304.

[17] Dill, D. (1991), Implementing matrix mechanics in Mathematica: Determination of Clebsch-Gordan coefficients by matrix diagonalization, Compu. Phys. 6, 616-624.

[18] Emiliani, C., and N.J. Shackleton (1974), The Brunhes epoch: Isotopic paleotemperatures and geochronology, Science 183, 511-514.

[19] Engstrom, D.R., B.C.S. Hansen, and H.E. Wright (1990), A possible Younger Dryas record in Southeastern Alaska, Science 250, 1383-1385.

[20] Gasse, F., M. Arnold, J.C. Fontes, M. Fort, E. Gilbert and A. Huc (1991), A 13,000-year climate record from western Tibet, Nature 353, 742-745.

[21] Goldreich, P., and S.J. Peale (1970), The obliquity of Venus, Astron. J. 75, 273-284.

[22] Hansen, K.S. (1982), Secular effects of oceanic tidal dissipation on the Moon's orbit and the Earth's rotation, Rev. Geophys. Space Phys. 20, 457-480.

[23] Hargreaves, R. (1895), Distribution of solar radiation on the surface of the Earth and its dependence on astronomical elements, Trans. Camb. Phil. Soc. 16, 58-94.

[24] Hays, J.D., J. Imbrie, and N.J. Shackleton (1976), Variations in the Earth's orbit: Pacemaker of the ice ages, Science 194, 1121-1132.

[25] Herbert, T.D. and S.L. D'Hondt (1990), Precessional climate cyclicity in Late Cretaceous-Early Tertiary marine sediments: A high resolution chronometer of boundary events, Earth Plan. Sci. Lett. 99, 263-275.

[26] Hilgren, F.J. (1991) Extension of the astronomically calibrated time scale to the Miocene/Pliocene boundary, Earth Plan. Sci. Lett. 107, 349-368.

[27] Imbrie, J., and J.Z. Imbrie (1980), Modeling the climatic response to orbital variations, Science 207, 943-953.

[28] Ivins, E.R., C.G. Sammis, and C.F. Yoder (1992), Deep mantle viscous structure with prior estimate and satellite constraint, J. Geophys. Res. (submitted),.

[29] Kahn, M.I., T. Oba, and T.L. Ku, Paleotemperatures and glacially induced changes in oxygen-isotope composition of sea water during late Pleistocene and Holocene time, Geology 9, 485-490.

[30] Kinoshita, H. (1977), Theory of rotation of the rigid Earth, Celest. Mech. 15, 277-326.

[31] Kubo, Y. (1979), A core-mantle interaction in the rotation of the Earth, Celest. Mech. 19, 215-241.

[32] Laskar, J. (1986), Secular terms of classical planetary theories using the results of general theory, Astron. Astrophys. 157, 59-70.

[33] Laskar, J. (1988), Secular evolution of the solar system over 10 million years, Astron. Astrophys. 198, 341-362.

[34] Laskar, J. (1990), The chaotic motion of the solar system: A numerical estimate of the size of the chaotic zones, Icarus 88, 266-291.

[35] Laskar, J., T. Quinn, and S. Tremaine (1992), Confirmation of resonant structure in the solar system, Icarus 95, 148-152.

[36] Le Treut, H., and M. Ghil (1983), Orbital forcing, climate interactions, and glaciation cycles, J. Geophys. Res. 88, 5167-5190.

[37] Loper, D.E. (1975), Torque balance and energy budget for the precessionally driven dynamo, Phys. Earth Plan. Inter. 11, 43-60.

[38] Martinson, D.G., W. Menke, and P. Stoffa (1987), An inverse approach to signal correlation, J. Geophys. Res. 87, 4807-4818.

[39] Mathews, P.M. and I.I. Shapiro (1992), Nutations of the Earth, Ann. Rev. Earth Plan. Sci. 20, 469-500.

[40] Mathews, P.M., B.A. Buffet, T.A. Herring, and I.I Shapiro (1991), Forced nutations of the Earth: Influence of inner core dynamics, J. Geophys. Res. 96, 8219-8242.

[41] Merriam, J.B. (1988), Limits on lateral pressure gradients in the outer core from geodetic observations, Phys. Earth Plan. Inter. 50, 280-290.

[42] Milani, A.(1988), Secular perturbations of planetary orbits and their representation as series, in Long-term Dynamical Behavior of Natural and Artificial N-body Systems, A.E. Roy (ed), pp. 73-108, Reidel, Boston.

[43] Milankovitch, M. (1920), Theorie Mathematique des Phenomenes Thermiques Produits par la Radiation Solaire, Gauthier-Villars, Paris, 336 pp.

[44] Miskovic, V.V. (1931), Variations seculaires de elements astronomiques de l'orbite terrestre, Glas. Spr. Kral'yevske Akad. 143.

[45] Nakada, M., and K. Lambeck (1988), The melting history of the late Pleistocene Antarctic ice-sheet, Nature 333, 36-40.

[46] Nakiboglu, S.M. (1982), Hydrostatic theory of the Earth and its mechanical implications, Phys. Earth Plan. Inter. 28, 302-311.

[47] North, G.R. (1975), Theory of energy-balance climate models, J. Atmos. Sci. 32, 2033-2043.

[48] North, G.R. and J.A. Coakley (1979), Differences between seasonal and mean annual energy balance models, J. Atmos. Sci. 36, 1189-1204.

[49] North, G.R., R.F. Cahalan, and J.A. Coakley (1981), Energy balance climate models, Rev. Geophys. Space Phys. 19, 91-121.

[50] Olsen, P.E. (1986), A 40-million year lake record of Early Mesozoic orbital climatic forcing, Science 234, 842-848.

[51] Park, J., and K.A. Maasch (1992), Plio-Pleistocene time evolution of the 100-kyr cycle in marine paleoclimate records, J. Geophys. Res. (submitted).

[52] Peltier, W.R. (1982), Dynamics of the ice age Earth, Adv. Geophys. 24, 1-146.

[53] Platzman, G.W., G.A. Curtis, K.S. Hansen, and R.D. Slater (1981), Normal modes of the world ocean, J. Phys. Ocean. 11, 579-603.

[54] Poincare, H. (1910), Sur la precession des corps deformables, Bull. Astr. 27, 322-356.

[55] Quinn, T.R., S. Tremaine, and M. Duncan (1991), A three million year integration of the Earth's orbit, Astron. J. 101, 2287-2305.

[56] Raymo, M.E., W.F. Ruddiman, J. Backman, B.M. Clement, and D.G. Martinson (1989), Late Pliocene variation in northern hemisphere ice sheets and North Atlantic Deep Water circulation, Paleocean. 4, 413-446.

[57] Richardson, D.L., and C.F. Walker (1989), Numerical simulation of the nine-body planetary system spanning two million years, J. Astron. Sci. 37, 159-182.

[58] Roberts, P.H. (1972), Electromagnetic core-mantle coupling, J. Geomag. Geoelec. 24, 231-259.

[59] Rochester, M.G. (1962), Geomagnetic core-mantle coupling, J. Geophys. Res. 67, 4833-4836.

[60] Rochester, M.G. (1976), The secular decrease of obliquity due to dissipative core-mantle coupling, Geophys. J. 46, 109-126.

[61] Rotenberg, M., R. Bivins, N. Metropolis, and J.K. Wooten (1959), The 3-j and 6-j symbols, Technology Press, Cambridge.

[62] Ruddiman, W.F., and A. McIntyre (1981), The North Atlantic Ocean during the last deglaciation. Paleogeo. Paleoclim. Paleoecol. 35, 145-214.

[63] Ruddiman, W.F., M.E. Raymo, D.G. Martinson, B.M. Clement, and J. Backman (1989), Pleistocene evolution: Northern hemisphere ice sheets and the North Atlantic Ocean, Paleocean. 4, 353-412.

[64] Sabadini, R., D.A. Yuen, and P. Gasperini (1982), Polar wandering and the forced response of a rotating, multi-layered planet, J. Geophys. Res. 87, 2885-2903.

[65] Sasao, T., I. Okamoto, and S. Sakai (1977), Dissipative core-mantle coupling and nutational motion of the Earth, Publ. Astron. Soc. Japan 29, 83-105.

[66] Schatten, K.H., and J.A. Orosz (1990), Solar constant secular changes, Solar Phys. 125, 179-184.

[67] Shackleton, N.J., A. Berger, and R.W. Peltier (1990), An alternative astronomical calibration of the Lower Pleistocene timescale based on ODP Site 677, Trans. Roy. Soc. Edin. 81, 251-261.

[68] Sharaf, S.G., and N.A. Boudnikova (1967), Secular variations of elements of the Earth's orbit which influence climates of the geological past, Bull. Inst. Theor. Astron. 11, 231-261.

[69] Short, D.A., G.R. North, T.D. Bess, and G.L. Smith (1984), Infrared parameterization and simple climate models, J. Clim. Appl. Meteor. 23, 1222-1233.

[70] Short, D.A., J. G. Mengel, T.J. Crowley, W.T. Hyde, and G.R. North (1991), Filtering of Milankovitch cycles by Earth's geography, Quat. Res. 35, 157-173.

[71] Smith, M.L., and A.F.Dahlen (1981), The period and Q of the Chandler wobble, Geophys. J. 64, 223-281.

[72] Smylie, D.E., A.M.K. Szeto, and K. Sato (1990), Elastic boundary conditions in long period core oscillations, Geophys. J. Int. 100, 183-192.

[73] Spada, G., R. Sabadini, D.A. Yuen, and Y. Ricard (1992), Effects on post-glacial rebound from the hard rheology in the transition zone, Geophys. J. Int. 109, 683-700.

[74] Stacey, F.D. (1973), The coupling of the core to the precession of the Earth, Geophys. J. 33, 47-55.

[75] Stephens, G.L., G.G. Campbell, and T.H. Vonder Haar (1981), Earth radiation budgets, J. Geophys. Res. 86, 9739-9760.

[76] Stix, M. (1982), On electromagnetic core-mantle coupling, Geophys. Astrophys. Fluid Dynam. 21, 303-313.

[77] Taylor, K.E. (1984), Fourier representation of orbitally induced perturbations in seasonal insolation, in A.L. Berger et al. (eds) Milankovitch and Climate, 113-125, D. Reidel.

[78] Thomson, D.J. (1990), Quadratic inverse spectrum estimates: Applications to paleoclimatology, Phil. Trans. Roy. Soc. Lond. A332, 539-597.

[79] Toomre, A. (1966), On the coupling of the Earth's core and mantle during the 26,000-year precession, The Earth-Moon System, Plenum Press, pp. 33-45. Tushingham, A.M., and W.R. Peltier (1991), Ice-3G: A new model of late Pleistocene deglaciation based upon geophysical predictions of post-glacial relative sea-level change, J. Geophys. Res. 96, 4497-4523.

[80] Vernekar, A.D. (1972), Long period global variations of incoming solar radiation, Meteor. Mono. 12, 1-22.

[81] Vernekar, A.D. (1977), Variations in insolation caused by changes in orbital elements of the Earth, in The Solar Output and Its Variations, O.R. White (ed), pp. 117-130, Colo. Assoc. Univ. Press.

[82] Voorhies, C.V. (1991), Coupling an inviscid core to an electrically insulating mantle, J. Geomag. Geoelec. 43, 131-156.

[83] Ward, W.R. (1974), Climatic variations on Mars, 1. Astronomical theory of insolation, J. Geophys. Res. 79, 3375-3381.

[84] Ward, W.R. (1979), Present obliquity oscillations of Mars: Fourth-order accuracy in orbital e and I, J. Geophys. Res. 84, 237-241.

[85] Ward, W.R., and W.M. DeCampli (1979), Comments on the Venus rotation pole, Astrophys. J. Lett. 230, 117-121.

[86] Williams, G.E (1989a), Late Precambrian tidal rhythmites in South Australia and the history of the Earth's rotation, J. Geol. Soc. Lond. 146, 97-111.

[87] Williams, G.E. (1989b), Precambrian tidal sedimentary cycles and the Earth's paleorotation, Eos Trans. A.G.U. 70, 33-41.

[88] Williams, J.G., X X Newhall, and J.O. Dickey (1991), Luni-solar precession: Determination from lunar laser ranges, Astron. Astrophys. 241, L9-L12.

[89] Wu, P. (1990), Deformation of internal boundaries in a viscoelastic earth and topographic coupling between the mantle and core, Geophys. J. Int. 101, 213-231.

[90] Wu, P., and W.R. Peltier (1984), Pleistocene deglaciation and the Earth's rotation: A new analysis, Geophys. J. 76, 753-791.

[91] Wunsch, C. (1986), Dynamics of the North Sea pole tide reconsidered, Geophys. J. 87, 869-884.

[92] Wyant, P.H., A. Mongroo, and S. Hameed (1988), Determination of the heat transport coefficient in energy-balance climate models by extremization of entropy production, J. Atmos. Sci. 45, 189-193.

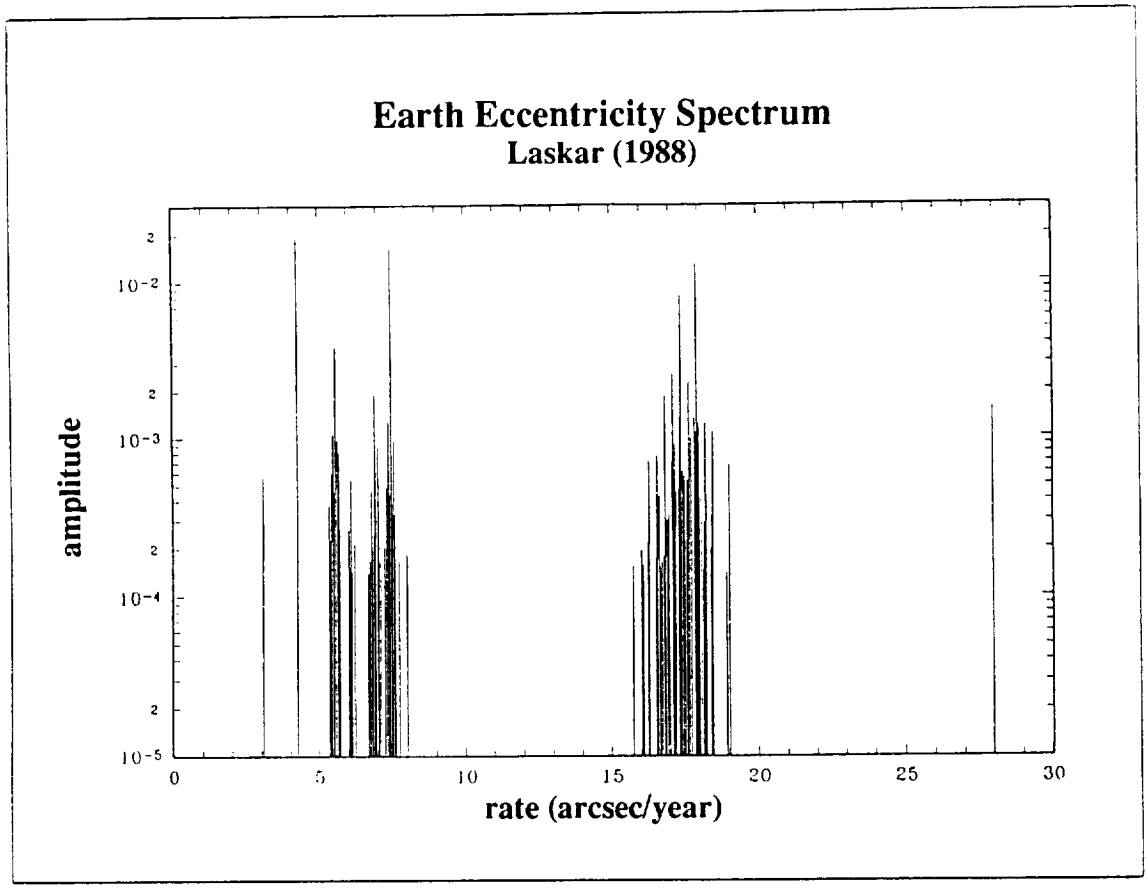

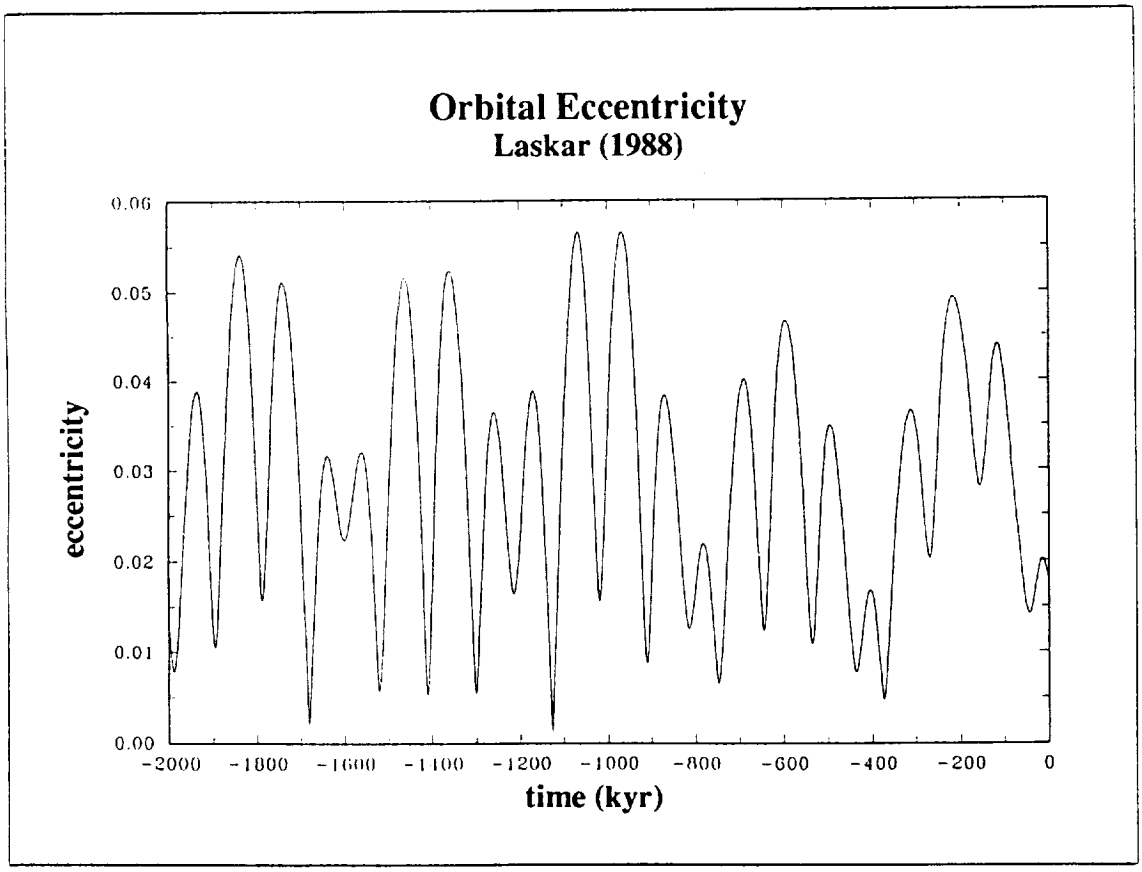

Figure 1
Orbital eccentricity spectrum and time series.
Both are based on the secular variation model of Laskar (1988).

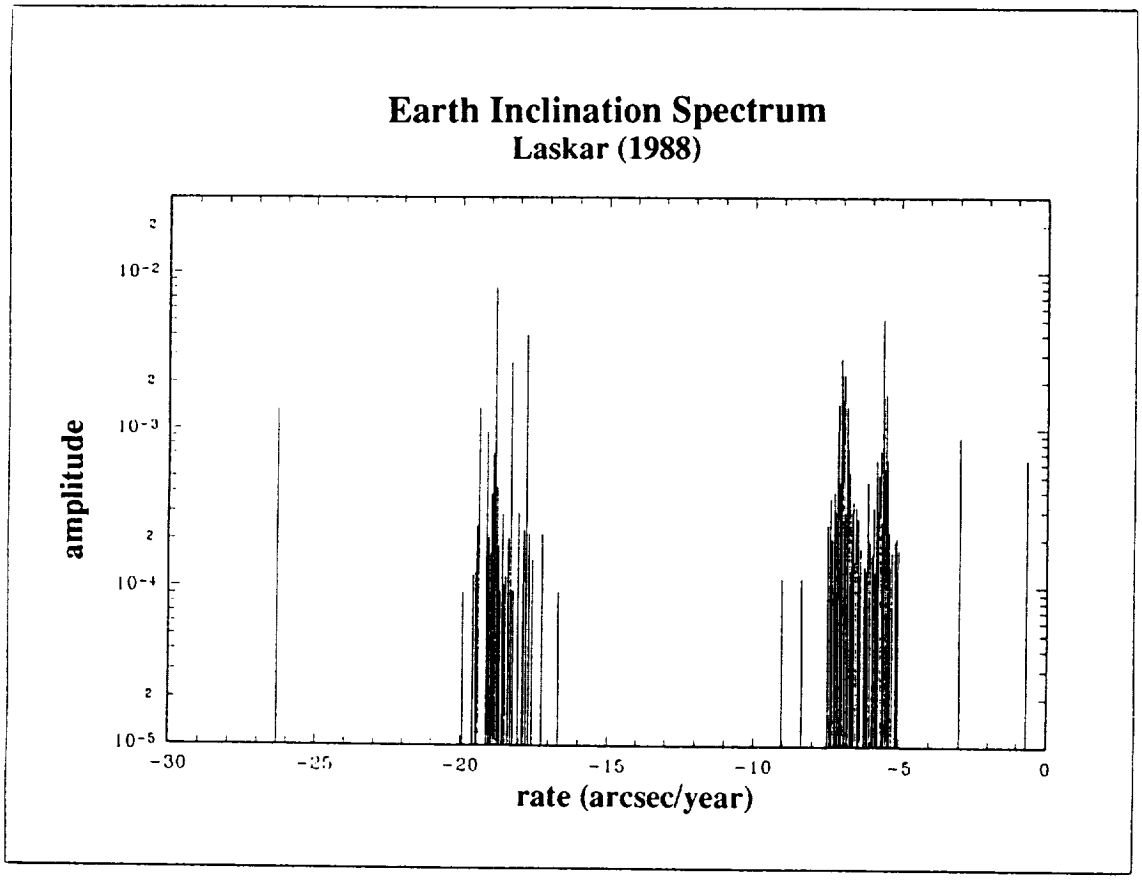

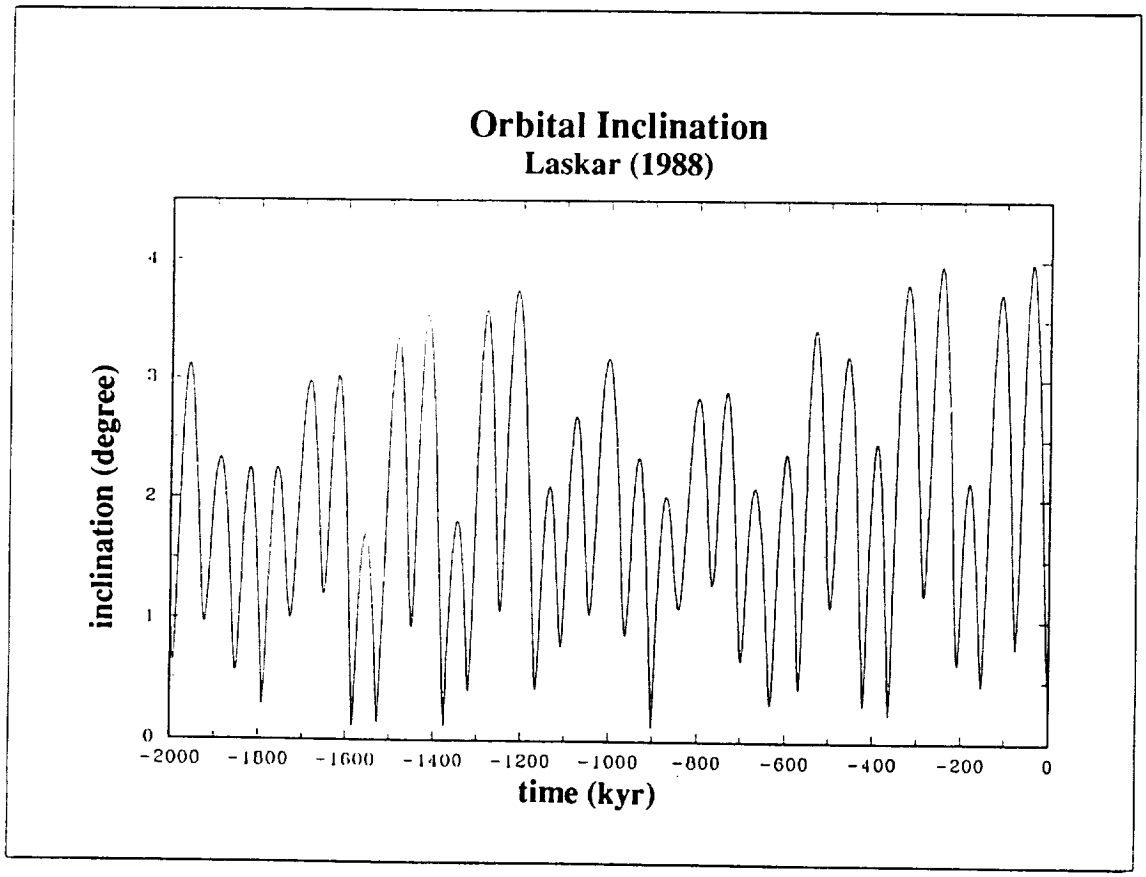

Figure 2
Orbital inclination spectrum and time series.
Both are based on the secular variation model of Laskar (1988).

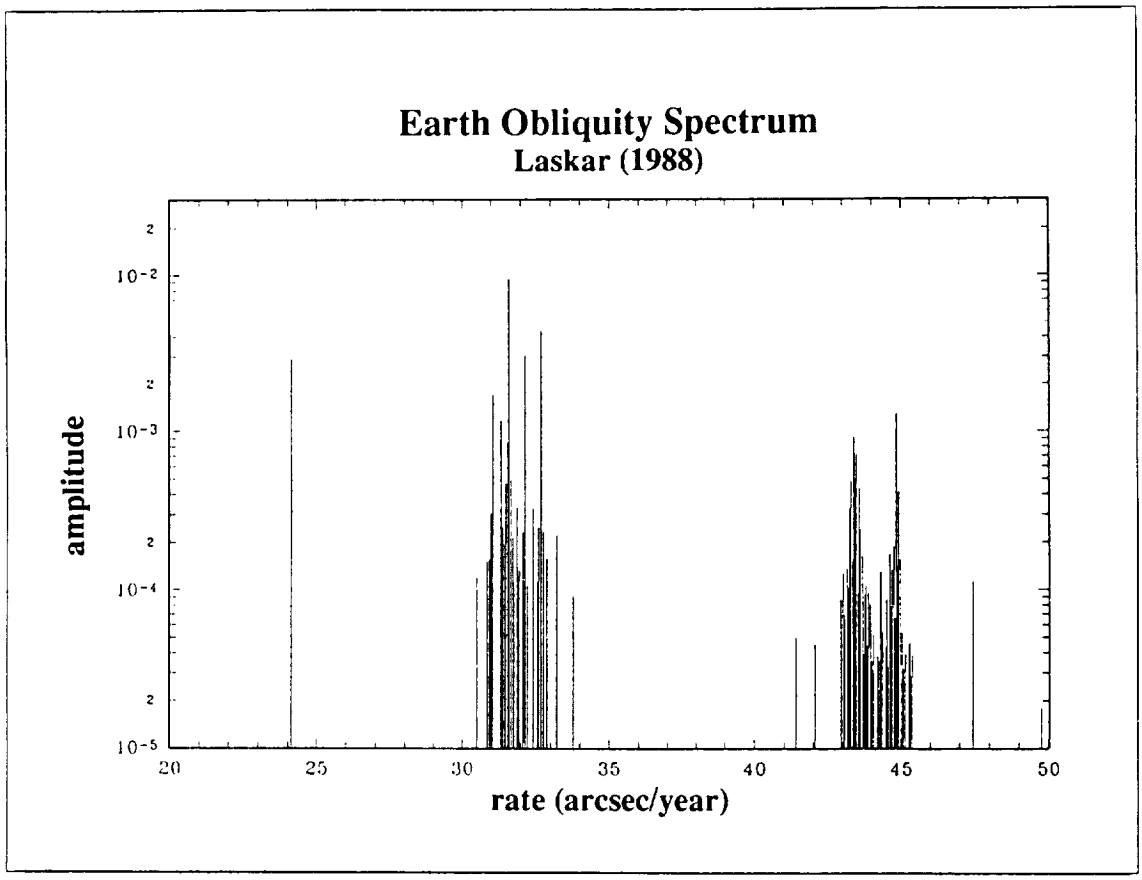

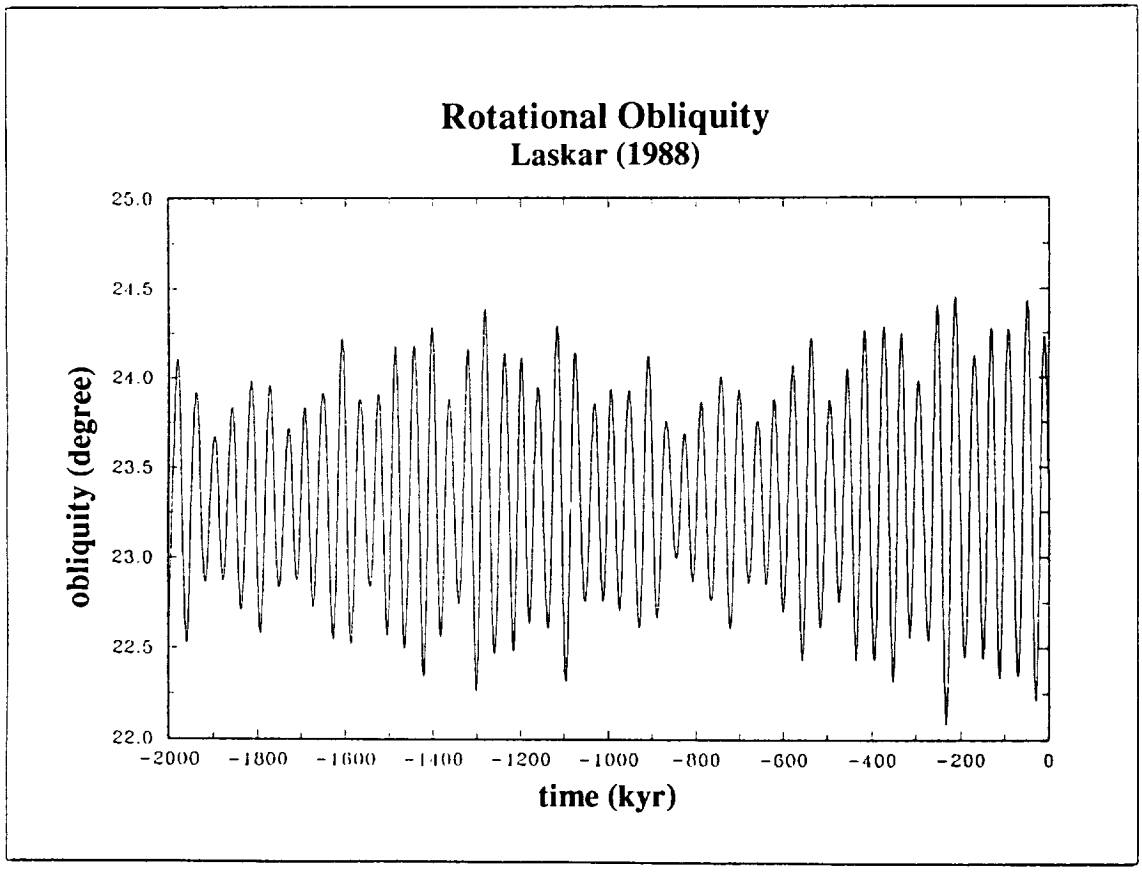

Figure 3

Rotational obliquity spectrum and time series.

Time series is based on rotational theory of Kinoshita (1977) and orbital model of Laskar (1988).

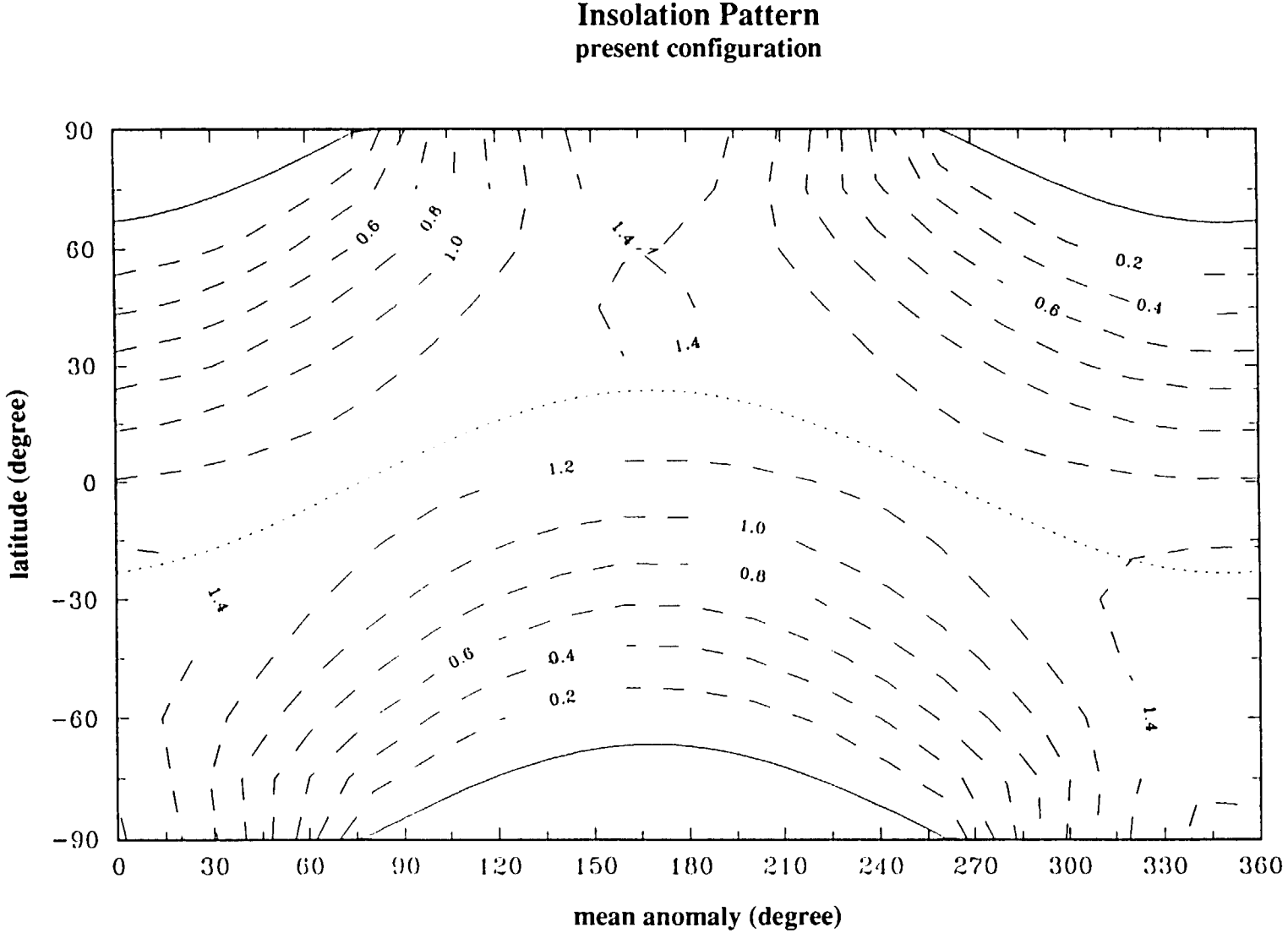

Figure 4
Latitudinal and Seasonal Insolation Pattern.

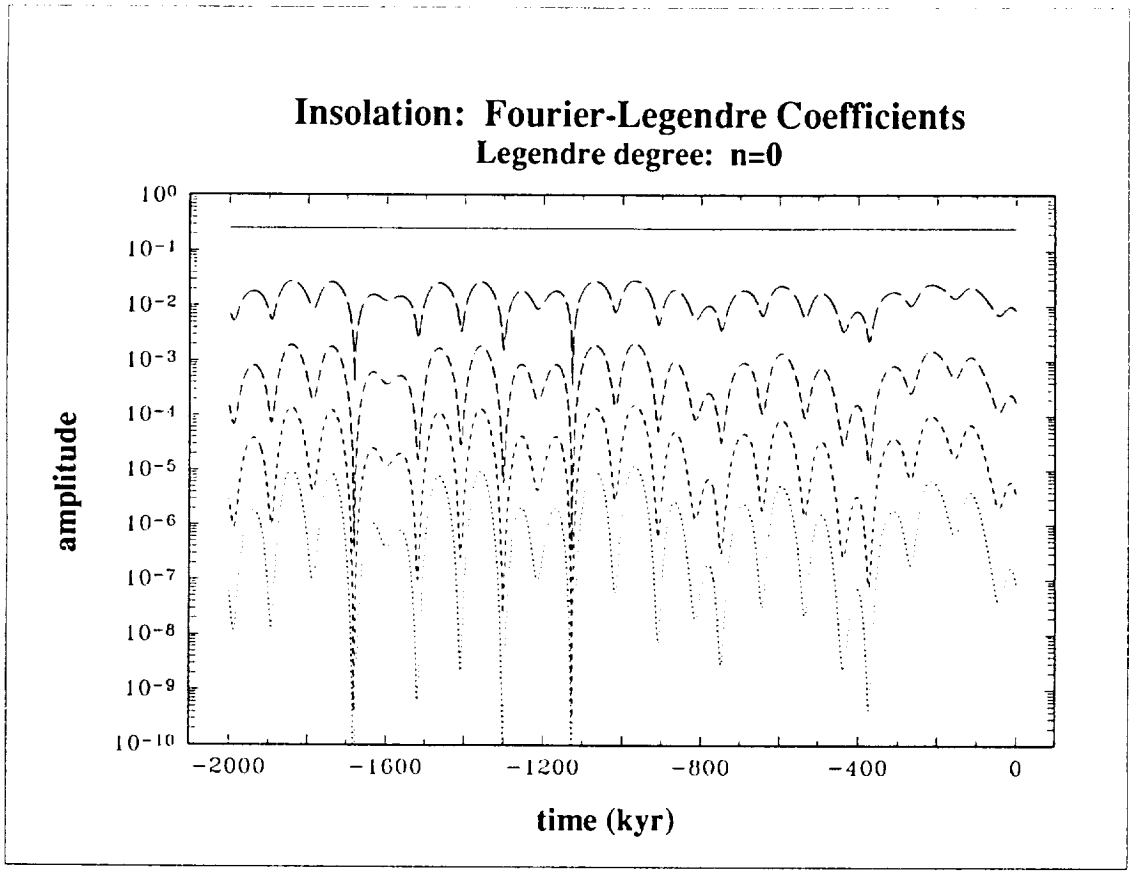

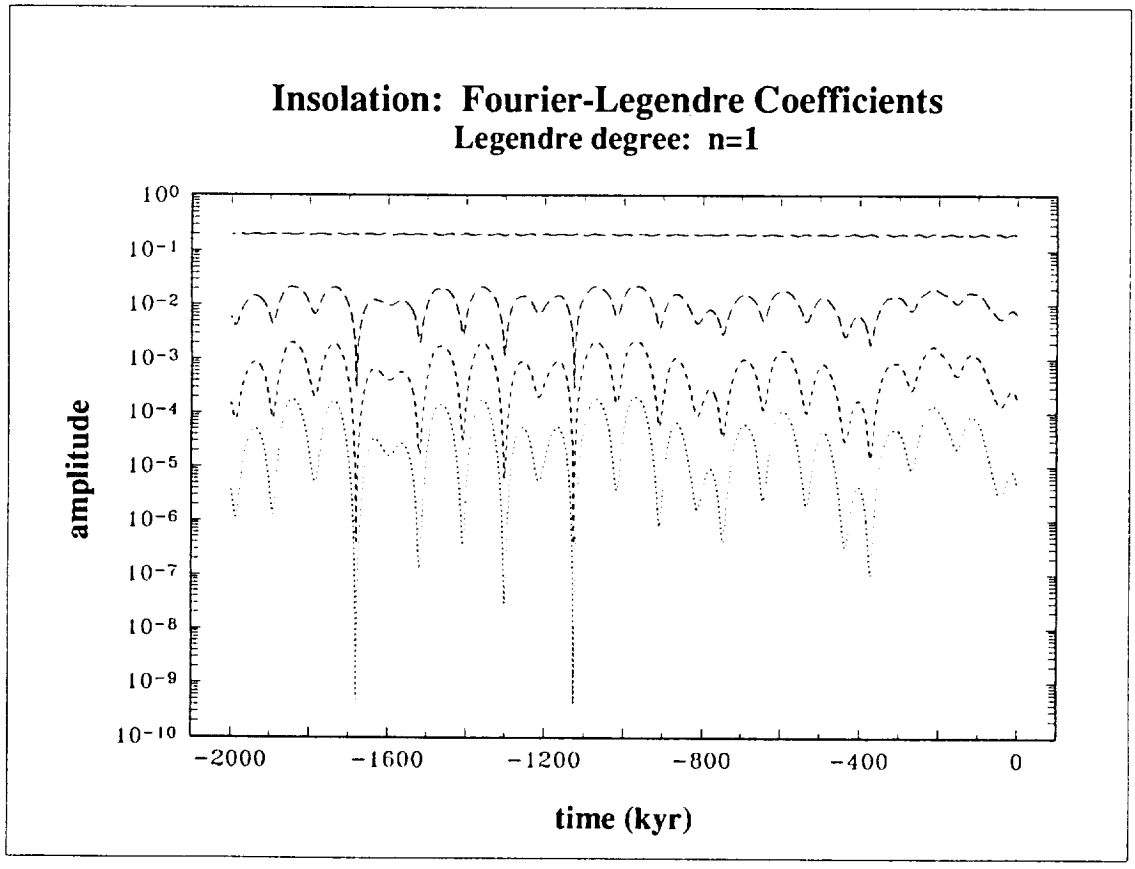

Figure 5a
Insolation Pattern Fourier-Legendre Coefficient Time Series.

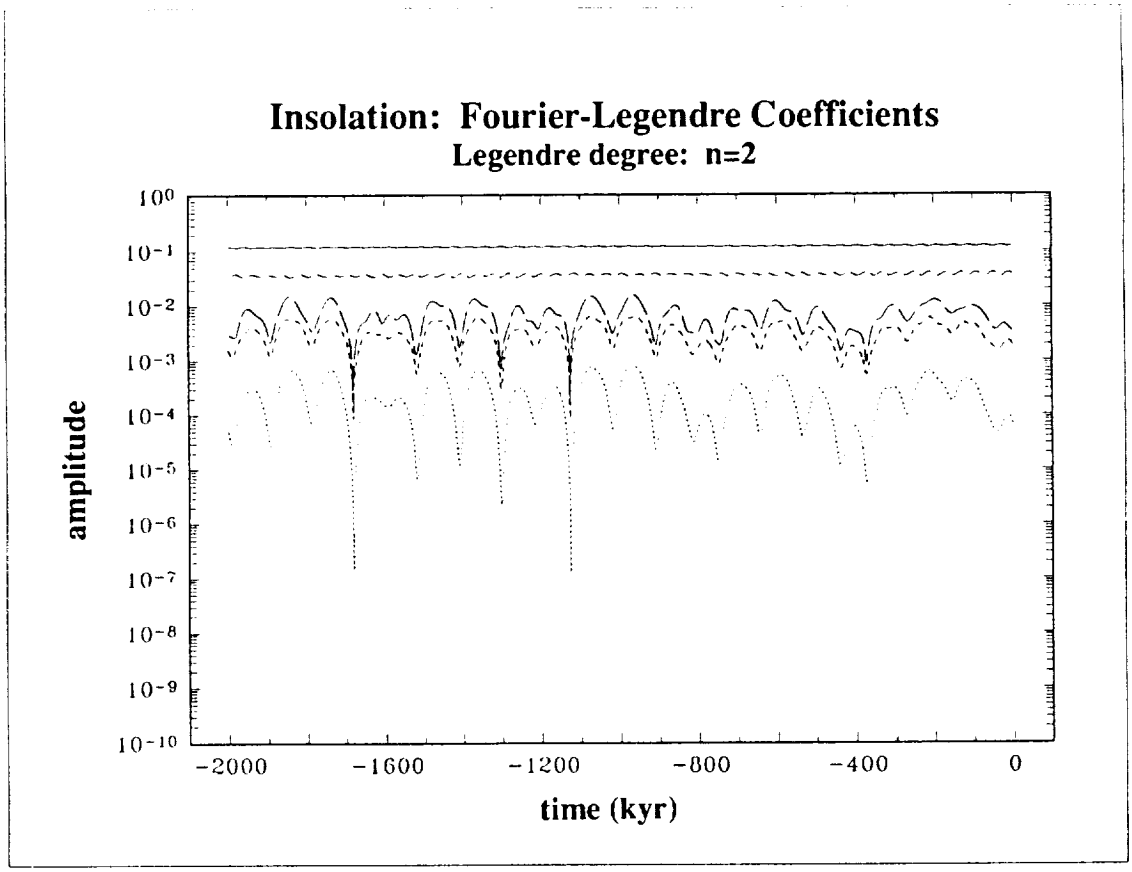

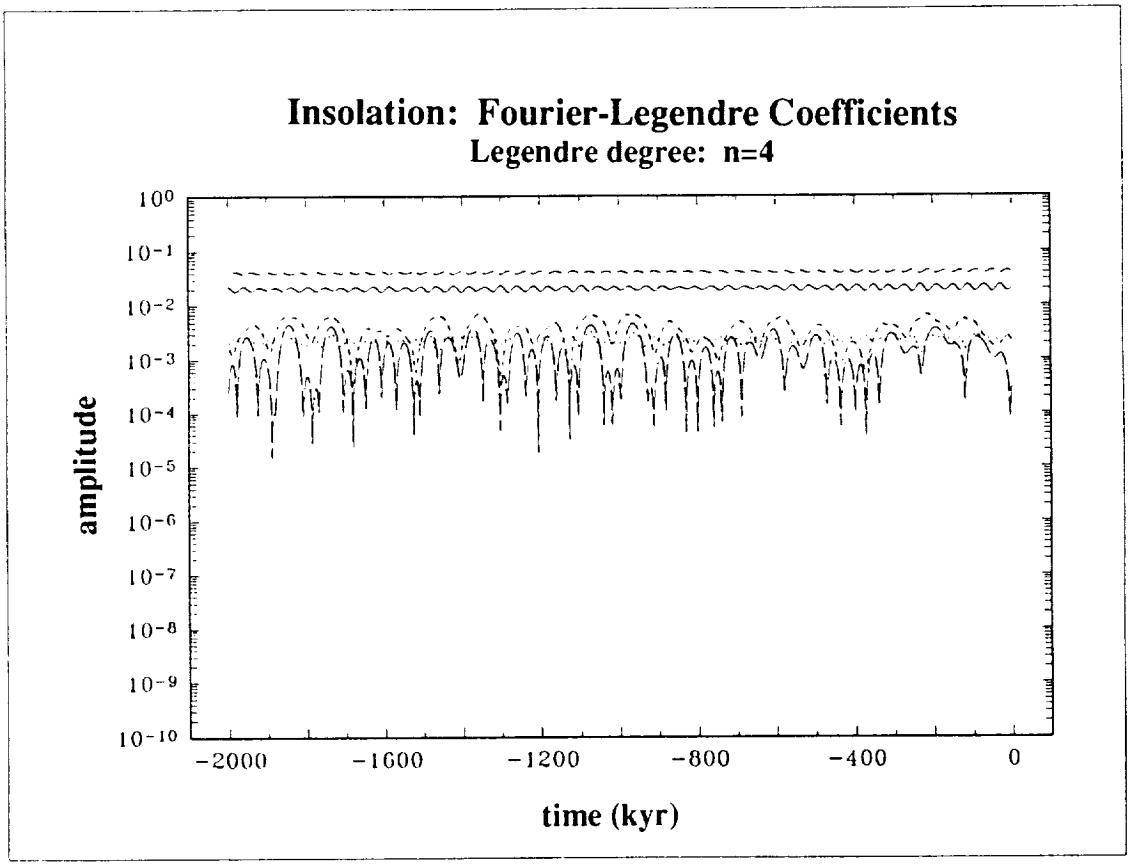

Figure 5b
Insolation Pattern Fourier-Legendre Coefficient Time Series.

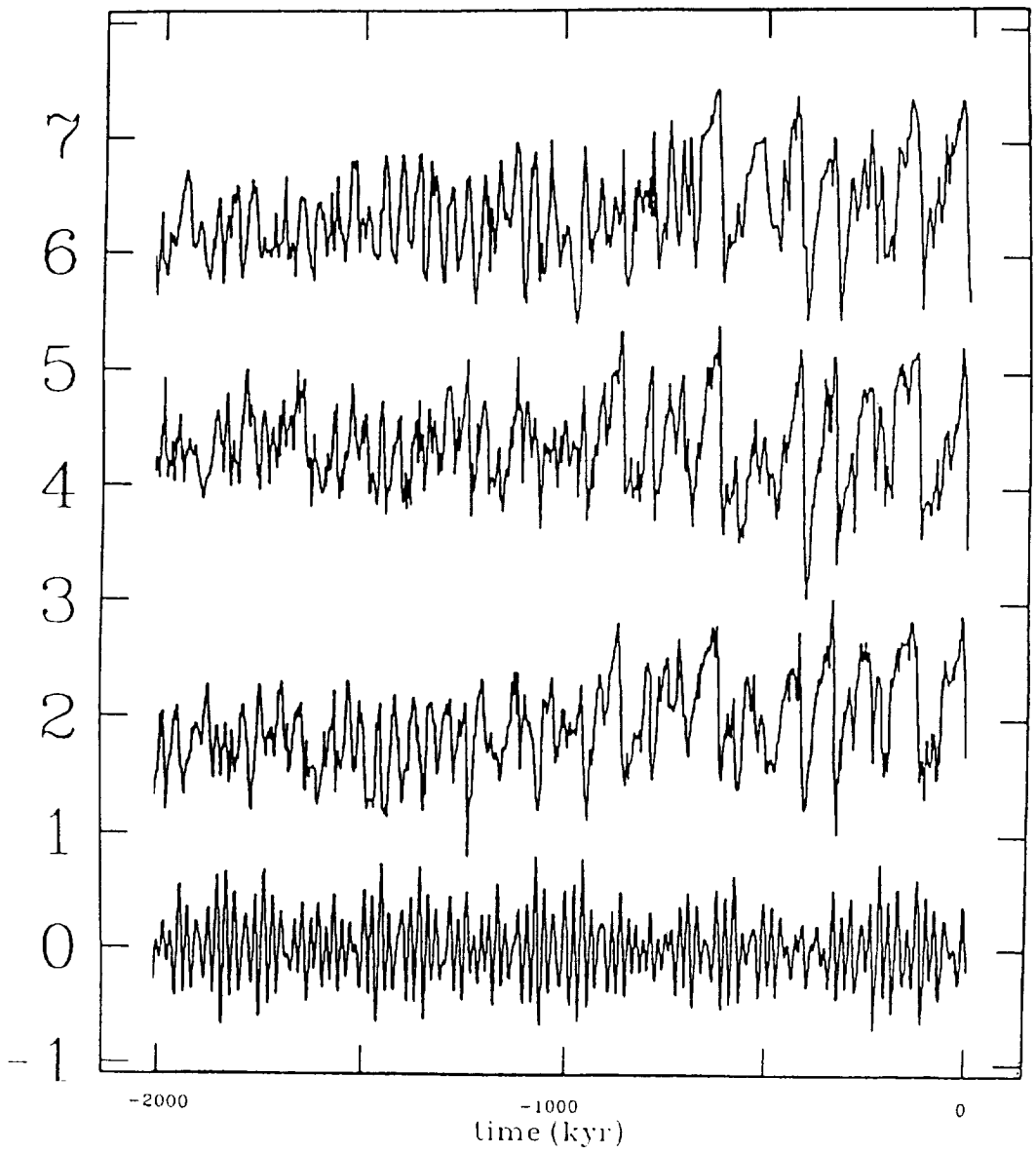

Figure 6
Paleoclimate Proxy Records and Insolation Time Series.
Curves are (top to bottom): DSDP 607 (benthic), ODP 677 (planktonic), ODP 677 (benthic), 65^{o} N insolation